Liquid Structure of Carbon Tetrachloride and Long-range Correlation

Keiko NISHIKAWA* and Yoshitada MURATA†

Department of Chemistry, Faculty of Science, Gakushuin University, Mejiro, Toshima-ku, Tokyo 171

(Received May 20, 1978)

The diffraction of liquid CCl_4 was measured by using the energy-dispersive X-ray diffractometer. The fine structure was observed for the first time in the present study. The existence of the fine structure in the diffraction pattern shows the long-range correlation "directly." The bcc cluster model for liquid CCl_4 is presented on the basis of the long-range correlation. The calculated intensity of the model is in good agreement with the observed one.

We constructed an energy-dispersive X-ray diffractometer using a solid state detector for the determination of liquid structure. The details were reported in a previous paper.[1)]

The energy-dispersive method has various merits in comparison with the traditional angle-dispersive method. First, a higher resolution of the s-value ($s=4\pi \sin\theta/\lambda$, λ: wavelength, 2θ: scattering angle) can be obtained. The resolution of the s-value is determined by the following equation:

$$\Delta s/s = \Delta E/E + \cot\theta \cdot \Delta\theta. \quad (1)$$

In the energy-dispersive diffractometer, the first term on the right side of Eq. 1 is nearly 0.01 and much larger than in a conventional angle-dispersive one. The second term in the angle-dispersive one, on the other hand, is several times as large as that in the energy-dispersive one. Since $\cot\theta \cdot \Delta\theta$ is less than 0.01 in our apparatus, the resolution $\Delta s/s$ is consequently a half of that in the conventional angle-dispersive diffractometer. Second, in the energy-dispersive method the scattering intensity is hardly affected by fluctuation in the primary beam intensity. Thirdly, it is possible to expand the observable region of the s-value, and hence the intensity data over the range of $s=0.15$—30 Å^{-1} can be obtained by our energy-dispersive X-ray diffractometer. Fourth, such accessories as a sample holder operated at high or low temperature can be mounted easily, since the design of the diffractometer is simple.

The scattering intensity from liquid CCl_4 was measured by taking advantage of the energy-dispersive method. Carbon tetrachloride has been studied well by the angle-dispersive method,[2-7)] and several models for liquid CCl_4 have been proposed by Narten *et al.*,[5)] Egelstaff *et al.*,[9)] Reichelt *et al.*[6)] and Narten.[7)] We reported the scattering intensity of liquid CCl_4 and its electron radial distribution function in a previous paper,[1)] but the analysis of the data obtained by energy-dispersive method was described mainly. In the present study it is shown that liquid CCl_4 has a long-range correlation at room temperature. A new model which explains the observed scattering intensity and the long-range correlation is presented.

Scattering Intensity and Radial Distribution Function

Details of the measurement and data analysis were described elsewhere.[1)] The absorption and Compton correction are more difficult in the energy-dispersive method than in the angle-dispersive one and these may be thought to be a demerit in energy-dispersive diffractometry, but these difficulties were resolved.[1)] The reduced intensity $i(s)$ was obtained in electron units after these corrections. The weighted structure function $si(s)$ is shown in Fig. 1 and agrees fairly well with the recent data for CCl_4 obtained by Narten[7)] except for the fine structure.

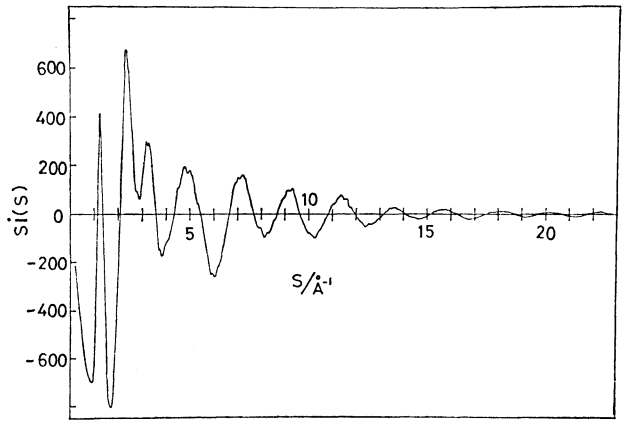

Fig. 1. Weighted structure function $si(s)$ for liquid CCl_4 at room temperature.

The electron radial distribution function from which the bulk density is subtracted, $4\pi r^2(\rho-\rho_0)$, is obtained by the Fourier transformation of $si(s)$,

$$4\pi r^2(\rho-\rho_0) = \frac{2r}{\pi \sum_j Z_j^2} \sum_s si(s) \cdot \sin(sr) \cdot \Delta s, \quad (2)$$

where ρ is the radial distribution function, ρ_0 the bulk density and Z_j the atomic number of a component atom j. The radial distribution function derived from Eq. 2 includes the distribution of the electron cloud. The

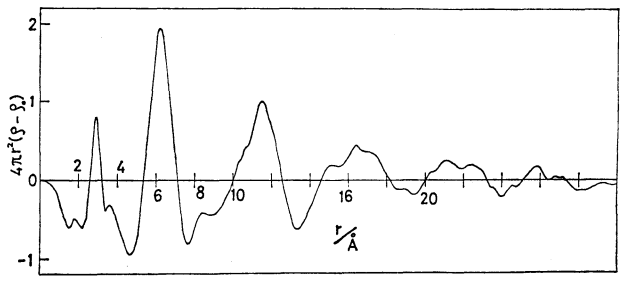

Fig. 2. Electron radial distribution function from which the bulk density was subtracted, $4\pi r^2(\rho-\rho_0)$.

† Present address: The Institute for Solid State Physics, The University of Tokyo, Roppongi, Minato-ku Tokyo 106.

Table 1. Intramolecular distances and associated root mean-square amplitudes
The values in parentheses indicate the standard deviations.

i	j	r_{ij}(Å)	l_{ij}(Å)	Reference	
C	Cl	1.768(6)	0.069(9)	Present work	(liquid)
		1.773(3)	0.079(9)	Ref. 5	
		1.767(3)	0.055(8)	Ref. 6	
		1.766(3)	0.043(4)	Ref. 7	
		1.765(2)	0.051(2)	Ref. 8	(gas)
Cl	Cl	2.889(2)	0.086(6)	Present work	(liquid)
		2.896(5)	0.092(3)	Ref. 5	
		2.886	0.070(9)	Ref. 6	
		2.884	0.078(3)	Ref. 7	
		2.886(2)	0.070(1)	Ref. 8	(gas)

electron radial distribution function of CCl_4 at room temperature is shown in Fig. 2.

The intramolecular parameters of CCl_4 were obtained by the least-squares fit of the calculated intensity of the free molecule to the observed intensity of the liquid at s-values larger than 8 Å^{-1}. These parameters are listed in Table 1 with those obtained by other experiments.[5-8] The interatomic distances are in good agreement with each other within experimental errors.

The Fine Structure in the Scattering Intensity and the Long-Range Correlation

Figure 2 shows that liquid CCl_4 at room temperature has long-range correlation. The information on the long-range correlation in liquid is confined in the region of $s<2$ Å^{-1}, but it is also recognized elsewhere. Figure 1 shows that the intensity curve has fine structure of short periodicity at small s-values.†† The fine structure near the top and the bottom of the halos at $s=3.2$ and 4.7 Å^{-1} was reproducible not only in repeated measurements but also in measurements at different scattering angles. The separation between the peaks in this fine structure were 0.2—0.3 Å^{-1}, which was larger than the estimated resolution in the s-value ($\Delta s=0.14$ Å^{-1} at those s-values) in our experiment. The difference between the collected counts at the top and the bottom of these small waves was about 500 counts, which were larger than the statistical random error ($\sqrt{n}=170$, where total counts $n=3\times10^4$). In the energy-dispersive method, the scattering intensity is hardly affected by fluctuations of the incident beam intensity. Therefore, the statistical random error given by the square root of the total counts at each position is the main origin of the noise.

To examine the relation between the fine stricture and the long-range correlation in liquid CCl_4, the inverse Fourier transformation of the experimental data was conducted. Each peak in the observed radial distribution function was expressed approximately by

$$G(r) = A\exp[-4(\ln 2)(r-r_0)^2/w^2] - B, \quad (3)$$

where A is the peak height measured from the average values at the minimum points, w the full width at half maximum, and B the difference between the zero line and the average minimum values. Figure 3 shows the curve for the inverse Fourier transformation for each Gaussian function $G(r)$. The curve (1), (2), (3), (4), (5), and (6) in Fig. 3(a) correspond to the peaks at the maximum positions $r_0=3.8$, 6.3, 8.3, 11.4, 16.3, and 21.5 Å, respectively. The summation of these curves is

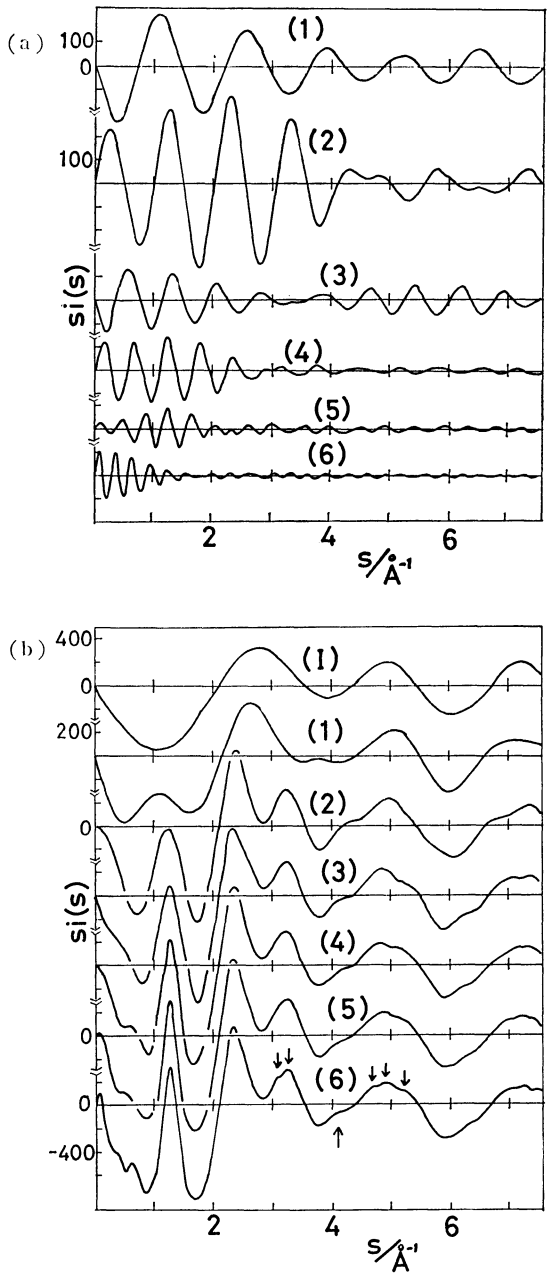

Fig. 3. (a) The inverse Fourier transformation function of the Gaussian function given by Eq. 3. Curves (1), (2), (3), (4), (5), and (6) correspond to the functions with $r_0=3.8$, 6.3, 8.3, 11.4, 16.3, and 21.5 Å, respectively. (b) The uppermost curve (I) is the inverse Fourier transformation function of the intramolecular part. Curve (n) is the sum of curves (1), (2)—(n) of Fig. 3(a) and curve (I).

†† The fine structure at large s-values is random noise, since the ratio of the reduced intensity $i(s)$ to the total scattering intensity is small.

shown in Fig. 3(b). The uppermost curve (I) is the inverse Fourtier transformation of the intramolecular contribution. Curve (n) in Fig. 3(b) represents the sum of curves (1), (2),$\cdots$(n) of Fig. 3(a) and curve (I). The fine structure indicated by the small arrows is in good agreement with the experimental intensity (Fig. 1), *e.g.*, the shoulder peak on the left side of the fourth halo, at $s\simeq 4$ Å^{-1}, appears due to the peaks at $r_0=6.3$ and 8.3 Å. The two small waves on the top of the third halo at $s\simeq 3.2$ Å^{-1} may be due to the scattering intensities corresponding to peaks at $r_0=16.3$ and 21.5 Å.

It has been concluded that the long-range correlation is not caused by experimental error nor by errors in the data analysis and this is supported by the following consideration. The electron radial distribution function, $4\pi r^2(\rho-\rho_0)$, computed using the intensity data obtained by Narten[7] shows a long-range correlation similar to Fig. 2. However, fine structure was not been observed in the intensity data. The fine structure represents "directly" that the molecules in the liquid phase have a long-range order in the arrangement. The presence of this fine structure had never been detected until the energy-dispersive method was applied to liquids in the present experiment.

Structure of Liquid CCl_4

The molecular arrangement in liquid CCl_4 was drawn on the basis of the following experimental results; (1) the small peak around 3.8 Å in the electron radial distribution function shows the nearest neighbor distance between chlorine atoms belonging to different molecules, and (2) the peaks with respect to the long-range correlation of molecular arrangement appear at integral multiples of about 5.7 Å, *i.e.* $r_0=11.4$, 16.3, and 21.5 Å. The peak at 3.8 Å is assigned to the Cl–Cl pair in the partial distribution function derived from X-ray and neutron diffractions by Narten.[7] That the peaks appear in equal intervals may show that CCl_4 molecules are arranged linearly. Consequently it is assumed that the three-fold axes of the CCl_4 molecules are linear. A chlorine atom of one molecule lies in the hollow formed by the three off-axis chlorine atoms of the other molecules. The distance between chlorine atoms belonging to different molecules is 3.8 Å, as shown in Fig. 4(a). Moreover, it is assumed that the average orientation is set in the eclipsed form for the chlorine atoms. In this arrangement, molecules form a body-centered cubic lattice, hereafter called a bcc cluster model. Since the nearest neighbor distance between chlorine atoms is 3.8 Å, the nearest neighbor distance referred to the molecular centers, *i.e.* the carbon atoms, is given by 5.77 Å and the second nearest neighbor distance is 6.77 Å, which corresponds to the lattice constant of the bcc lattice. Figure 4(b) shows the bcc cluster containing 15 CCl_4 molecules. The packing shown in Fig. 4(a) is similar to the "Apollo model" presented by Egelstaff *et al.*[9] They assumed that both molecules were freely oriented about the three-fold axes. However, neither the scattering intensity nor the distribution function was calculated for this model.

Of course, the liquid can never be the crystal. The

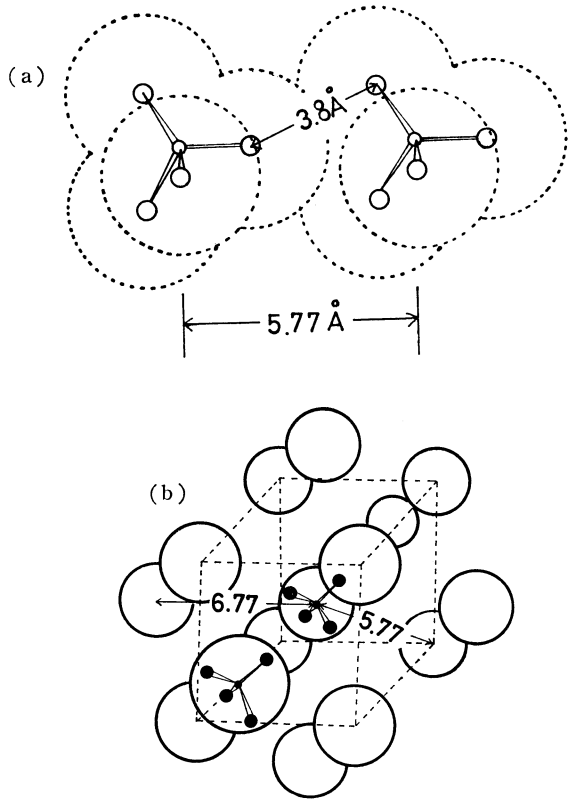

Fig. 4. (a) Packing model for liquid CCl_4. Small circles denote carbon atoms and large circles chlorine atoms. Van der Waals spheres of chlorine atoms are shown by dotted circles. (b) The bcc cluster model for liquid CCl_4 with 15 molecules. CCl_4 molecules are shown by circles. The orientation of all molecules is same as that described in the circles. The cube shown by broken lines forms the bcc unit cell.

molecule in the liquid phase lies around the equilibrium position, which forms the cluster. The cluster must have the same density as the actual liquid. We never mean that clusters with a density different from uniform medium exist actually—here "cluster" means a representation of the region where one molecule "feels" the "structure." The cluster is not rigid, but the structure becomes gradually loose as the molecules separate from the center of the cluster, *i.e.* the distance between molecules in the cluster is smeared as they are separated from each other. The smearing effect is treated with the increase of the root mean-square amplitude l_{ij} of the interatomic distance r_{ij}. The structure outside the cluster is a uniform medium.

The reduced intensity function may be computed from the equation,

$$i(s)=\frac{1}{N}\sum\sum_{i\neq j}f_if_j\frac{\sin(sr_{ij})}{sr_{ij}}\exp(-l_{ij}^2s^2/2)+i_c, \qquad (4)$$

where N is the number of CCl_4 molecules contained in the cluster. In the cluster model, the first term series in Eq. 4 must be terminated at the end of the cluster. The second term in Eq. 4 complements a fault due to this termination. This correction corresponds to placing a uniform and structureless medium outside the cluster. This is depicted in Fig. 5. The sphere surrounded by

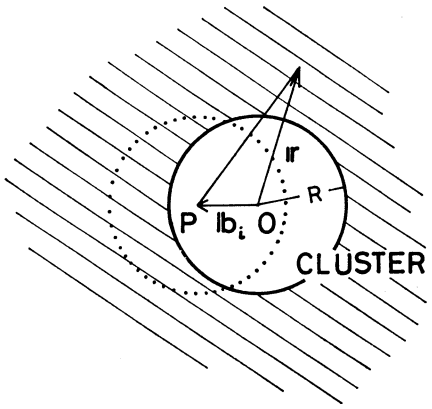

Fig. 5. A schematic illustration of the model used for the calculation of the correction term i_c in the reduced intensity $i(s)$.

the solid line is the cluster, in which the structure exists and the stripped region is the uniform medium. The continuous medium of the unit volume has a scattering factor $\langle F\rangle\rho_0$, where ρ_0 is the number density of CCl_4 in the liquid and $\langle F\rangle$ is the average scattering factor of CCl_4 in the continuous medium. The scattering intensity due to interference between the cluster and the continuous medium becomes,

$$i_c = \frac{1}{N}\sum_i\{f_i\langle F\rangle\rho_0 \exp(-l_i^2s^2/2)\int\exp(i(\boldsymbol{s}\cdot\boldsymbol{r}-\boldsymbol{b}_i))\mathrm{d}v_r\}, \quad (5)$$

where the origin is taken at the center of the cluster, $\boldsymbol{b}_i$ is the position vector of the i-th atom with a scattering factor f_i and l_i is the root mean-square amplitude of b_i. The integration in Eq. 5 is performed beyond the sphere of the cluster to infinity, that is over the stripped region of Fig. 5. The average scattering factor $\langle F\rangle$ is given by

$$\langle F\rangle = f_C + 4f_{Cl}\frac{\sin(sr_{C-Cl})}{sr_{C-Cl}}. \quad (6)$$

In Eq. 5 the atom around the periphery of the cluster effectively "feels" a much smaller cluster size than the atom at the center. On the other hand, the cluster means the representation of the region where one molecule "feels" the "structure." All molecules in the liquid must sit at the center of the cluster, when the second term of Eq. 4 is estimated. The surrounding of a molecule in a liquid is spherically symmetric except for near positions, and then the cluster radius R should be the same for all molecules. When the i-th atom is located at P (Fig. 5), the second term of Eq. 4 is integrated over the continuous medium beyond the dotted sphere. Therefore, it is reasonable to modify Eq. 5:

$$\begin{aligned} i_c &= \frac{1}{N}\sum_i f_i\langle F\rangle\rho_0\langle\exp(-is\cdot b_i)\rangle\exp(-l_i^2s^2/2) \\ &\quad\times\int_R^\infty \exp(i\boldsymbol{s}\cdot\boldsymbol{r})\mathrm{d}v_r \\ &= -\frac{1}{N}\sum_i f_i\langle F\rangle\rho_0\frac{\sin(sb_i)}{sb_i}\exp(-l_i^2s^2/2) \\ &\quad\times\frac{4\pi}{s^3}[\sin(sR)-sR\cos(sR)]. \end{aligned} \quad (7)$$

This equation is an extension of the formula derived by Warren.[10]

With a cluster radius R equal to 8.4 Å, the best agreement between the calculated and experimental intensities was obtained. This value, 8.4 Å, is reasonable, since the effective radius of the cluster containing 15 CCl_4 molecules, namely, the distance between the center of the cluster and the farthest chlorine atom is 8.54 Å. The weighted structure function, $si(s)$, with respect to the bcc cluster model with 15 CCl_4 molecules was calculated and is shown over the range from $s=0$—6

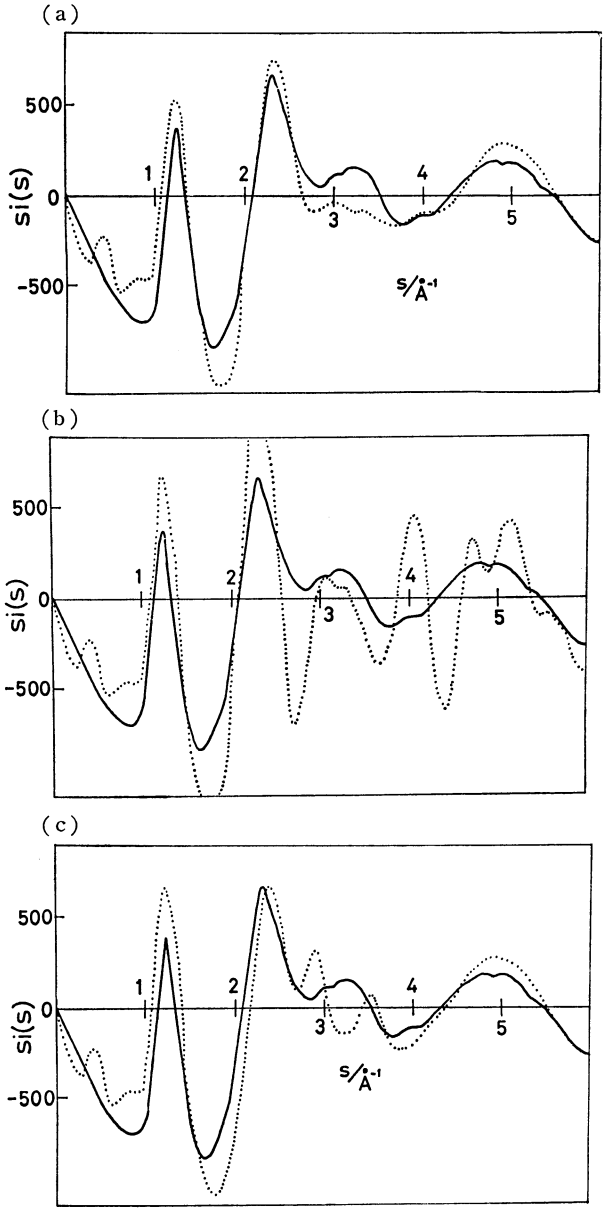

Fig. 6. Weighted structure function $si(s)$ for liquid CCl_4. (a) Solid line: experimental intensity. Dotted line: calculated intensity for the bcc cluster model with 15 CCl_4 molecules. (b) Solid line: experimental intensity. Dotted line: calculated intensity for the bcc cluster model neglecting the root mean-square amplitude. (c) Solid line: experimental intensity. Dotted line: calculated intensity for the bcc model modified by the freely rotating molecules.

Table 2. Root mean-square amplitudes assumed for the calculated intensity of Figs. 6(a) and (c)

r_{ij}(Å)	l_{ij}(Å)
1.77 (C–Cl, intramolecule)	0.069
2.89 (Cl–Cl, intramolecule)	0.086
3—4	0.25
4—6	0.30
6—8	0.35
over 8	0.40

Å^{-1} in Fig. 6(a). The intensity curve in s-values larger than 6 Å^{-1} is almost the same as that of the free molecule of CCl_4. The full line is the observed intensity, and the dotted line shows the calculated intensity, where the root mean-square amplitude l_{ij} used is listed in Table 2. The fine structure on the fourth halo does not appear in the dotted line in Fig. 6(a). However, if the smearing effect is neglected, that is, l_{ij} is assumed to be zero in Eq. 4, the fine structure appears as shown in Fig. 6(b). The periodicity in the calculated intensity agrees well with the fine structure of the experimental intensity indicated by the full line. Therefore, the molecular arrangement of the bcc cluster explains the fine structure in the scattering intensity.

The dotted line in Fig. 6(c) corresponds to the bcc cluster model modified by the freely rotating molecules. In the model of the free rotation, the halo at 3.3 Å^{-1} splits into two peaks at 2.9 and 3.6 Å^{-1}, which differs from the experimental intensity. The possibility of a free rotation model is excluded by the distance between the nearest neighbor molecules, 5.77 Å, which is smaller than the van der Waals diameter of CCl_4, 7 Å. Consequently the barrier is too high for the molecule to rotate independently.

In the calculated intensity two small peaks appear at s=0.4 and 0.9 Å^{-1} as shown by the dotted line in Fig. 6(a) and this represents a discrepancy between the calculated and observed intensities. These peaks are, however, not significant. The intensity calculated by use of only the first term of Eq. 4 agrees well with the dotted line of Fig. 6(a) in the region of $s>1$ Å^{-1}. On the other hand, the second term of Eq. 4 dominates the region of s=0—1 Å^{-1}. In this region the weighted intensity curve without i_c has a strong peak, as shown by the solid line in Fig. 7. The dotted line in Fig. 7 shows the correction term, $-si_c$. These large values were subtracted in the calculation of the reduced intensity in the region of s=0—1 Å^{-1}.

The calculated intensity of the bcc cluster model is in good agreement with the observed intensity, not only in the main peaks at $s\simeq 1.2$ and 2.3 Å^{-1} but also in the fine structure around s=3—4 Å^{-1} (Fig. 6(a)). However disagreement in the intensity around s=3 Å^{-1} was observed. This discrepancy may be caused by the analysis, since it is difficult to derive the reduced intensity $i(s)$ from the total scattering intensity in this region.[1] Further possible source of the discrepancy may be the small cluster size and the large root mean-square amplitude assumed in this model.

In the present model, the peak in the radial distribution at 6.3 Å consists of two kinds of radial distances refering to the molecular centers, 5.77 and 6.77 Å, in which 8 and 6 molecules are contained, respectively. The equal interval in the peak in the radial distribution, *i.e.* 5.77, 11.4, 16.3, and 21.5 Å, is explained from the bcc cluster model.

The first and second nearest neighbor distances of the molecular center, 5.77 and 6.77 Å, happen to coincide with the model presented by Narten *et al.*,[5] as shown in Table 3 in spite of a different model. Narten *et al.* assumed at first the "crystal" of the space group Pa3,

Table 3. The distance between molecular centers r and the number of the pair n in the two models of liquid CCl_4

bcc cluster model		Pa3 model	
r(Å)	n	r(Å)	n
5.77	8	5.77	6
6.77	6	6.13	1
		6.77	6

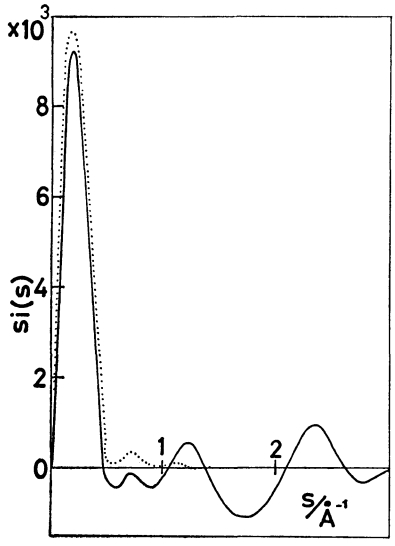

Fig. 7. The effect of the correction of Eq. 7. The full line is the weighted intensity neglecting the correction term i_c. The dotted line shows the correction term, $-si_c$.

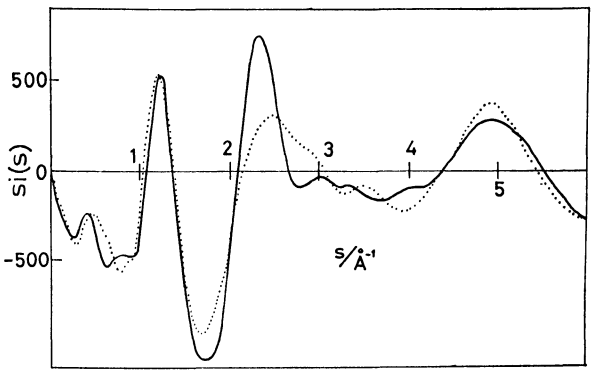

Fig. 8. Weighted structure function for liquid CCl_4. Solid line: bcc cluster model with 15 CCl_4 molecules. Dotted line: Pa3 model with 14 CCl_4 molecules.

which is the space group in the close-packing structure of Group IV halides *e.g.* SnI_4.[11] Next, the "ideal structure" was distorted by the least-squares fit to the observed diffraction data of the liquid. In order to compare the bcc cluster model with the distorted close-packing model, $si(s)$ of the close-packing model (Pa3 model) was calculated using Eq. 4 and the parameters given by Narten *et al.* The result is shown in Fig. 8 together with the intensity calculated from the bcc model. The agreement between both intensities fairly well in the positions of the main peaks, but differences exist in the region $s \simeq 2.5$—3.5 Å^{-1} and in the fine structure. Therefore, the long-range correlation demonstrated by the present study is important for estimating the liquid structure, and the measurements including the fine structure are necessary. For this purpose the energy-dispersive method is superior to the angle-dispersive one.

We are indebted to Prof. T. Iijima of Gakushuin University for helpful disscussions and reading of the manuscript. The present work was partially supported by Grant-in-Aid for Scientific Research from the Ministry of Education.

References

1) Y. Murata and K. Nishikawa, *Bull. Chem. Soc. Jpn.*, **51**, 411 (1978).
2) A. Eisenstein, *Phys. Rev.*, **63**, 304 (1943).
3) E. E. Bray and N. S. Gingrich, *J. Chem. Phys.*, **11**, 351 (1943).
4) R. W. Gruebel and G. T. Clayton, *J. Chem. Phys.*, **46**, 639 (1967).
5) A. H. Narten, M. D. Danford, and H. A. Levy, *J. Chem. Phys.*, **46**, 4875 (1967).
6) G. Reichelt, J. U. Weidner, and W. Zimmermann, *Ber. Bunsenges. Phys. Chem.*, **78**, 1050 (1974).
7) A. H. Narten, *J. Chem. Phys.*, **65**, 573 (1976).
8) Y. Morino, Y. Nakamura, and T. Iijima, *J. Chem. Phys.*, **32**, 643 (1960).
9) P. A. Egelstaff, D. I. Page, and J. G. Powles, *Mol. Phys.*, **20**, 881 (1971).
10) B. E. Warren, *Phy. Rev.*, **45**, 657 (1934).
11) F. Meller and I. Fankuchen, *Acta Crystallogr.*, **8**, 343 (1955).